JOURNAL OF Materials CHEMISTRY

Formation of $YBa_2Cu_3O_{7-\delta}$ superconducting films by electrodeposition

Marisol S. Martín-González, Javier García-Jaca, Emilio Morán and Miguel Á. Alario-Franco*

Grupo de Estado Sólido, Departamento Química Inorgánica, Facultad de Ciencias Químicas, Universidad Complutense, 28040-Madrid, Spain. E-mail: maaf@eucmax.sim.ucm.es

Received 24th November 1998, Accepted 19th March 1999

Superconducting thick films of Y–Ba–Cu–O have been prepared *via* an electrodeposition procedure of the constituent metals on metallic substrates (Cu, Ag) followed by an oxidative thermal treatment. The films were electrodeposited at a constant potential of -3.5 V (*vs.* Ag/AgCl) from a single electrolyte bath, which contains the nitrates of the cations in dimethyl sulfoxide. The initial state of the precursor film and the formation process of the final superconducting film have been followed by IR spectroscopy, thermogravimetric analysis, X-ray diffraction and scanning electron microscopy. In the precursor film, yttrium and copper are present as metals while barium forms a carbonate. Dimethyl sulfoxide (DMSO) is not inert under the experimental conditions and oxidises to the sulfone. The superconducting transition temperature (T_c) of the final film was ≈ 92 K and the critical current density (J_c) values were $\approx 9\,500$ A cm^{-2} at 77 K and zero field, the highest so far obtained by electrodeposition.

Introduction

Since the discovery of high temperature superconductors in 1986[1] one of the major problems associated with such materials has been the difficulty in producing these brittle ceramics, as compared to metals, into usable configurations, for instance tapes or wires. These materials certainly have a promising future in technological applications as for example: energy transport without Joule effect losses (useful in engines, transformers, *etc.*), fabrication of high magnetic intensity solenoids (important in nuclear magnetic resonance, nuclear fusion or synchrotrons) and signal detection with minimal noise (relevent to electronics, telecommunications, computers, receiver/amplifiers). However, for this to become a reality, much progress has to be achieved in the formation and processing of superconducting films. An early approach was the so-called oxide powder-in-tube technique[2] (OPIT), in which a superconductor powder is placed inside a silver tube and swaged and/or rolled into the desired conductor shape. This method presents the drawback that when the tube had to be bended so as, for example, to make a solenoid, grain contact was often lost. Later, deposition of films was investigated using different procedures, such as:[3] (a) for *thin film* approaches: electron beam evaporation,[4] sputtering,[4,5] laser ablation[6] and chemical vapour deposition (CVD)[7] and (b) for *thick film* solution approaches: solution-spraying, sol–gel processing and electrochemical methods.[8–20]

In the latter type of approach, the high temperature superconducting (HTSC) film is not directly produced, but first a precursor film is obtained which it is then fired at high temperatures to sinter the particles. The thin film approach usually requires the use of a single crystal substrate and vacuum technology, but an advantage of these approaches is that a certain degree of epitaxial growth is often achieved. Among these techniques, the synthesis of superconducting films *via* electrochemical methods has some advantages, such as (i) economic favourability owing to its low cost, (ii) fast deposition rates, (iii) easy technology transfer because of it being well established in the electronic and metallurgical industry, for example, in protective applications and (iv) not requiring ultrapure starting materials, (v) possibility of covering different shapes and size coatings on different substrates.

The cathodic electrodeposition process has been successfully employed for the preparation of superconductors such as Y–Ba–Cu–O,[8–13] Bi–Sr–Ca–Cu–O,[14–16] Tl–Ba–Ca–Cu–O,[17,18] Ba–K–Bi–O[19] and Hg–Ba–Ca–Cu–O.[20] However, to our knowledge, the available information about the process in going from the precursor film to the final superconducting one is scarce. However, such information is very useful for the optimisation of the quality of films and for controlling their growth.

In a previous article, the study was focused on the Bi–Sr–Ca–Cu–O system.[15] The present work deals with the synthesis and characterisation of the precursor, the formation process, its influence on the morphology and covering of the film and the superconducting properties of thick $YBa_2Cu_3O_{7-\delta}$ films obtained from electrodeposited precursors on several metallic substrates.

Experimental

The process used was chronoamperometry carried out using a conventional three electrode cell: the working electrode was a sheet of a conducting silver (0.5×1 cm) or copper (0.5×0.5 cm) foil, the reference electrode was Ag/AgCl and platinum was used as a counter electrode. In order to optimise the adherence of the film to the surface, the copper foil was polished with sand paper then washed with ultrapure water and afterwards with the solution. For the silver foil, previous studies have proved[15] that the detrimental influence of water on the covering, adherence and quality of the deposits can be very much diminished by careful cleaning of the silver surface, for example, using Al_2O_3 as an abrasive and then washing it several times. The electrolytic bath consisted of (Table 1) a solution in which the nitrates of the cations are dissolved in dimethyl sulfoxide (DMSO, Aldrich) which were used as received. All the reagents were of a purity grade higher than 99%. The electrolytic bath contains also a small quantity of water (<1%), introduced through the hydrated salts and as an impurity in the DMSO (≈ 0.2 wt%).

In order to determine the optimal concentrations of cations in solution yielding the desired composition on the electrode, a preliminary study of the deposit composition in relation to the concentration of copper and barium in the solvent was carried out. The potential was fixed at -3.5 V (*vs.* Ag/AgCl) with a computer-controlled VersaStat potentiostat/galvanostat Model 253. The copper nitrate concentration in solution was fixed at 20 mM and the barium nitrate concentration was varied. It was then determined that, to obtain a Ba : Cu ratio

Table 1 Synthesis conditions for the $YBa_2Cu_3O_{7-\delta}$ phase

Solvent	Bath composition	Deposition conditions (*vs.* Ag/AgCl)	Average current density/A cm^{-2}
DMSO (<1% H_2O)	$Y(NO_3)_3$ 20 mM $Ba(NO_3)_2$ 36 mM $Cu(NO_3)_2 \cdot 3H_2O$ 44 mM	dc Chronoamperometry $E = -3.5$ V for 30 min $T = 25$ °C	≈ -14

of 2:3 in the electrode (for $YBa_2Cu_3O_{7-\delta}$), the Ba:Cu ratio should be ≈4:5 in solution. Consequently, a typical electrolytic bath for the growth of Y-123 films consisted of 20 mM Y^{3+}, 36 mM Ba^{2+} and 44 mM Cu in dimethyl sulfoxide (Table 1); this is similar to ratios used previously.[9] The temperature was fixed at 25 °C by means of a thermostatic bath (Clifton NE4-DCE PLUS). The electrodeposited alloy films were heated at 900 °C for 24 h in air and post-annealed in O_2 at 450 °C for 24 h.

Several techniques have been used in order to follow the film formation at different stages and to characterise the final deposit: (i) IR spectroscopy (Midac Prospect-IR), (ii) thermogravimetric analysis (TG) (Perkin Elmer Model 7), (iii) X-ray diffraction (Siemens D-501 diffractometer), (iv) scanning electron microscopy [JEOL JSM-6400 fitted with a LINK data acquisition system for energy dispersive X-ray spectra (EDS)], (v) magnetic susceptibility (LakeShore 7225 susceptometer operating in AC mode at 125 Hz with different magnetic fields in the temperature range 77–120 K) and (vi) measurement of critical current density (J_c) for zero magnetic field (commercial SQUID Quantum Design MPMS XL at 77 K and 5 K). J_c values were extracted from hysteresis loop measurements of the magnetisation *vs.* field. The external magnetic field in the hysteresis loops increased from zero to a maximum value (4.5 T) then decreased, reversing in sign and so forth. The critical current density in A cm^{-2} was obtained for a slab of planar geometry, where the film surface was parallel to the field applying the Bean model,[21] resulting in the expression:[22]

$$J_c = 20\frac{|-M_+ + M_-|}{D}$$

where M_+ and M_- are given in emu cm^{-3} and D (in cm) represents a length scale where shielding currents are supposed to circulate freely, which in a thin film, corresponds to the thickness.

It is important that the substrate does not diffuse in, or chemically react with the deposited film during the thermal treatment and that, even if it diffuses to a small extent, this should not alter the superconducting properties. For this reason, from the different substrates that were tested;[23,24] the final deposition was only carried out over either copper or silver since they gave the best results.

Results and discussion

1 Copper as substrate

Previous work, in which powders of different substrates and $YBa_2Cu_3O_{7-\delta}$ were mixed and pressed together into pellets, have shown that Cu reacts with $YBa_2Cu_3O_{7-\delta}$ at temperatures above 900 °C in air and that, in all cases, CuO and Cu_2O are formed.[25] In order to study the influence of this reaction in thick superconducting films, the morphology of films with copper as substrate was studied by SEM (Fig. 1). Interfaces Y–Ba–Cu–O/Cu–O/Cu^0 are shown in Fig. 1(a). It can also be observed that beneath the Y–Ba–Cu–O film there is a thick layer of CuO and, below the latter, the Cu foil remains as copper metal. The Y–Ba–Cu–O film [Fig. 1(b)] is not homogeneous owing to the presence of different phases: $YBa_2Cu_3O_{7-\delta}$, Y_2BaCuO_5 and CuO as detected by X-ray diffraction. Also, the film shows a degree of clustering due to intergrowth between Cu–O and Y–Ba–Cu–O layers [Fig. 1(c)]. This intergrowth is produced by the diffusion of copper from the copper substrate through the deposited

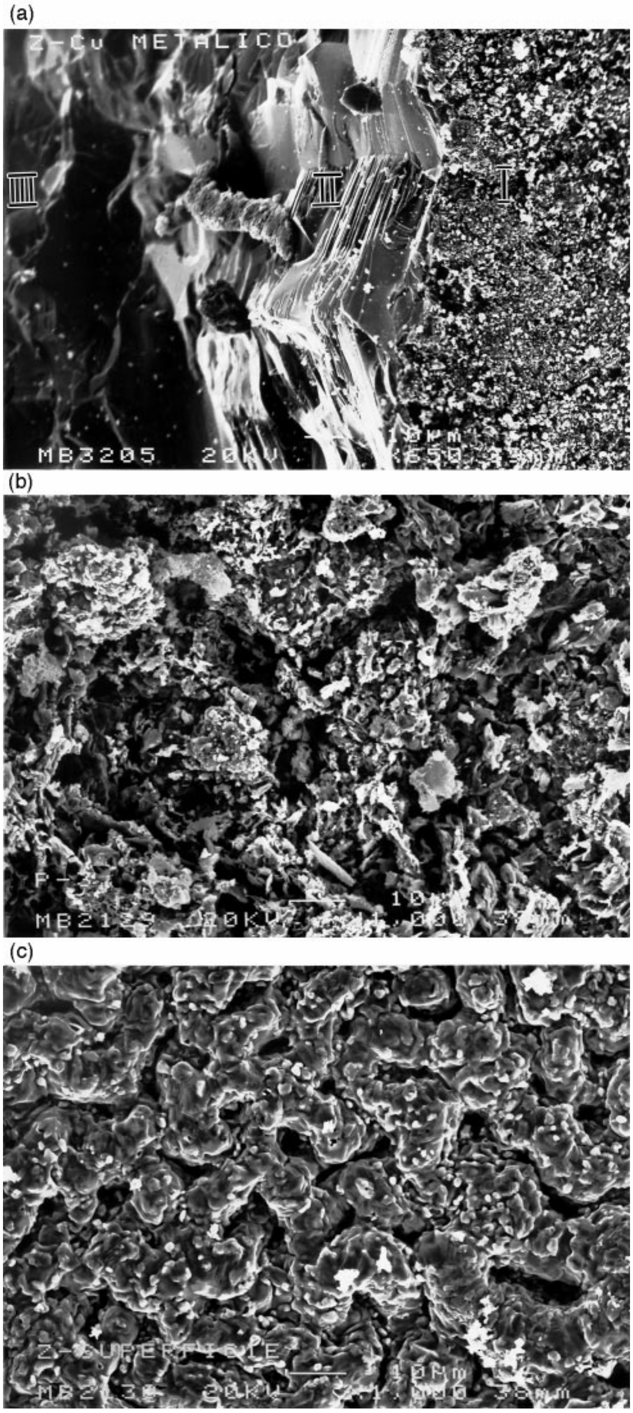

Fig. 1 Micrographs of Y–Ba–Cu deposits on copper foil treated at 900 °C. (a) the different layers after the thermal treatment: Y–Ba–Cu–O, Cu–O and Cu^0 are indicated by I, II and III, respectively, (b) morphology of the Y–Ba–Cu–O film and (c) interface Y–Ba–Cu–O/Cu–O.

Y–Ba–Cu film. This process supplies an important quantity of extra copper to the film, prevents a good connectivity between the superconducting particles and enhances the formation of impurities such as Y_2BaCuO_5, CuO, *etc.*

2 Silver as substrate

X-Ray and SEM studies show that upon high temperature oxidation of silver foil in air[25] the foils do not react with the superconductor so that silver constitutes an optimal substrate material for the deposition of precursor films and the subsequent thermal treatment. The films were studied, before thermal treatment, by IR spectroscopy (Fig. 2). The spectrum in Fig. 2 was taken immediately after the electrodeposition process. The bands observed can be assigned[26] as summarised in Table 2. The solvent bands disappear upon leaving the sample for two days in air. Although water is reduced to H_2 during the electrodeposition process, the presence of water in the electrolyte was found not to be critical below a certain limit and had a minimal effect if the substrate was adequately cleaned.[15] The presence of carbonates can be attributed to a reaction with atmospheric CO_2 during the preparation of the IR pellets.

All the IR spectra measured before thermal treatment showed a sharp strong band at 1384 cm^{-1} and a weak one at 1205 cm^{-1}. These bands were not eliminated upon leaving the film for two days in air; and can be assigned to ν_{as}(S=O) and ν_s(S=O), respectively, corresponding either to an alkyl sulfone (1340–1290 and 1165–1120 cm^{-1})[27,28] or an alkyl sulfonate (1415–1380 and 1200–1187 cm^{-1}).[27] Indeed, in some cases, the 1384 cm^{-1} band was the most intense band of the spectrum! This suggests that DMSO is not inert under our experimental conditions and undergoes a degree of oxidation.

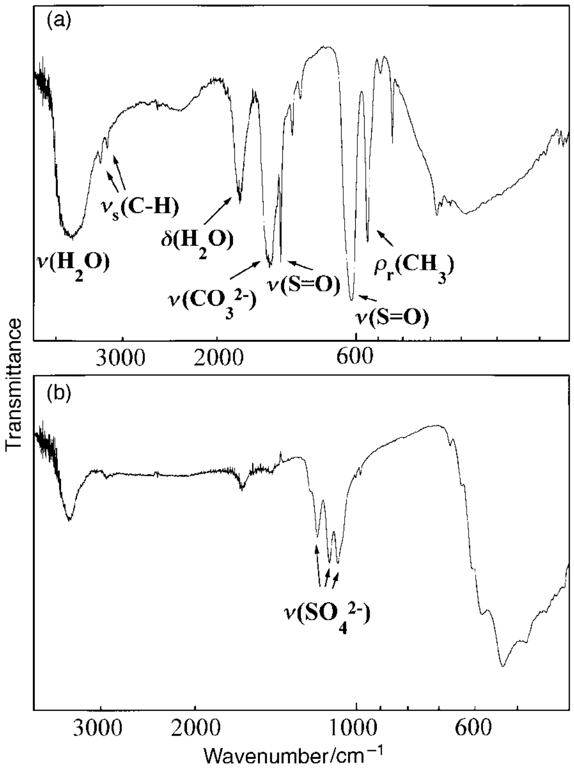

Fig. 2 IR spectrum of a Y–Ba–Cu deposit (a) taken immediately after the electrodeposition process and (b) after thermal treatment at 900 °C.

Table 2 IR spectra assignments

Chemical species	Band/cm^{-1}	Assignment[26]
DMSO	3008, 2917	ν_s(C–H)
	1317	$\nu_s(S–CH_3)$
	1022	ν(S=O)
	953	$\rho_r(CH_3)$
Water	3564	$\nu(H_2O)$
	1651	$\delta(H_2O)$
Carbonate	1455	$\nu(CO_3^{2-})$

In order to elucidate the phases present in the films, X-ray diffraction patterns of the Ag/Y–Ba–Cu–O films before thermal treatment were collected. Fig. 3(a) indicates the presence of Cu and Cu_2O and confirms that copper is electrodeposited as a metal. The presence of Cu_2O can be attributed to the partial oxidation of copper in air.[29] No diffraction maxima corresponding to either barium or yttrium phases were observed at this stage suggesting that these phases are essentially amorphous.

We have observed that by simply leaving the precursor films in air the quantity of DMSO in the final superconducting film can be diminished. For this reason, the study of the morphology and the thickness of these precursor films was carried out by SEM after leaving the films for two days in air. The advantages of this procedure are discussed elsewhere.[30] From the micrograph of the film shown in Fig. 4 its thickness is *ca.* 20 μm. The contact between the electrodeposited film and the substrate is made at multiple points, but the film is not well stuck to the substrate. This could be due to the fact that metal atoms often aggregate rather than evenly deposit on a foreign surface producing a dendritic growth.[31] In such a growth, some nuclei appear first, and, starting from those, the film grows generating a dendritic intergrowth in the final precursor film. It can also be observed on the same film that, after two

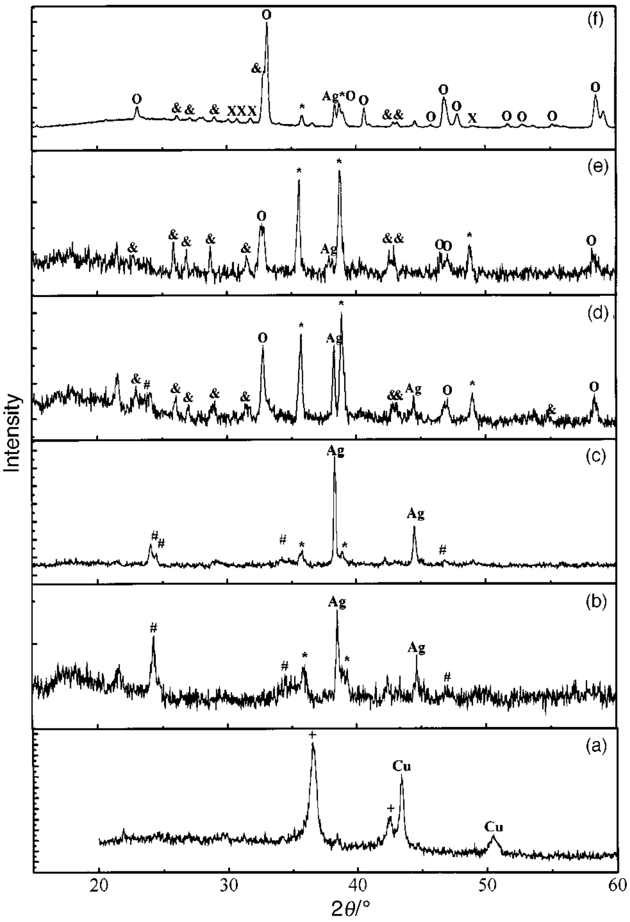

Fig. 3 X-Ray diffraction patterns of Y–Ba–Cu deposits treated at different temperatures: (a) fresh, (b) 500 °C, (c) 600 °C, (d) 700 °C, (e) 800 °C and (f) 900 °C. Identification marks: Cu_2O (+), $BaCO_3$ (#), CuO (*), $BaSO_4$ (&), Y_2BaCuO_5 (X) and $YBa_2Cu_3O_{7-\delta}$ (O).

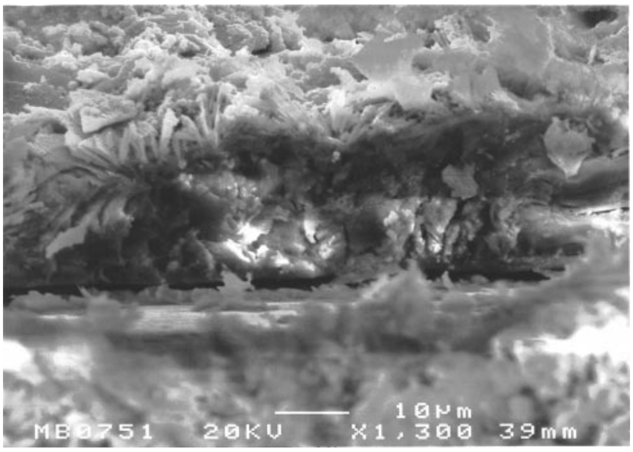

Fig. 4 Side view of the precursor Y–Ba–Cu film on silver foil.

days in air, the deposit is essentially formed by randomly oriented flakes, however, the coverage of the substrate is high.

The evolution of this initial film during the oxidation process was also studied by thermogravimetric analysis (Fig. 5). Three important thermogravimetric effects were observed in the derivative of the TG curve: around 260 and 380 °C, which correspond to weight gains, and at 740 °C, corresponding to a weight loss. The first weight gain (≈260 °C) can be assigned to the oxidation of Cu_2O, formed by previous oxidation of Cu to Cu_2O which happens almost at room temperature; Cu_2O is then stable up to 145 °C and its oxidation takes places slowly up to 179 °C and rapidly up to 285 °C;[29] the peak corresponding to this effect is always observed between 260 and 280 °C. The second weight gain (≈380 °C) can be interpreted knowing that: (a) yttrium metal is oxidised at *ca.* 400 °C in air,[29] (b) the maximum is always observed in the range 380–405 °C in different TG experiments and (c) this increment of weight was not observed when a thermogravimetric analysis of a Ba–Cu only sample was made. It can therefore be assumed that yttrium must be deposited as a *metal.*[32] The third thermogravimetric process (≈740 °C) can be assigned to the formation of the $YBa_2Cu_3O_{7-\delta}$ phase.

In order to confirm this hypothesis and to determine the evolution of the species during the thermal treatment of the film, they were heated at different temperatures in air in cumulative treatments and studied by both XRD (Fig. 3) and SEM (Fig. 6).

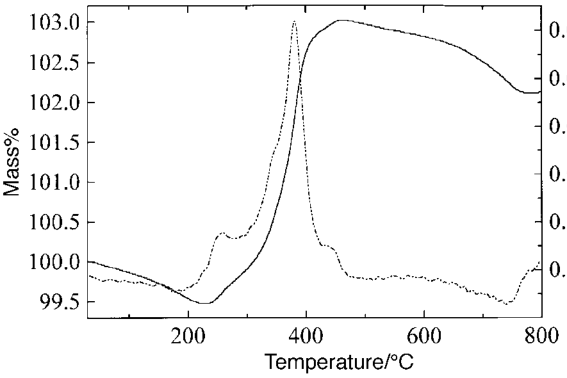

Fig. 5 Thermal behaviour of the electrodeposited Y–Ba–Cu material: (—) TG and (---) derivative curves.

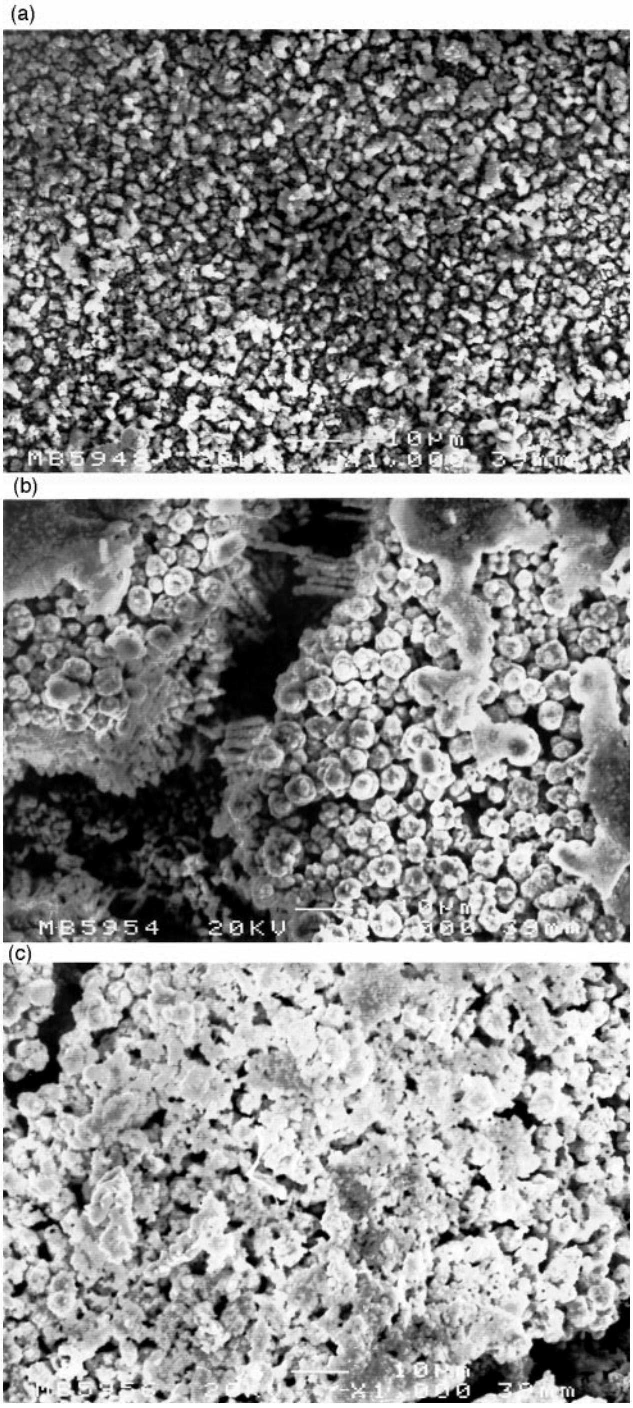

Fig. 6 Micrographs of Y–Ba–Cu deposits on silver foil treated at different temperatures: (a) 500 °C, (b) 700 °C and (c) 800 °C.

The X-ray diffraction pattern of the film heated at 500 °C [Fig. 3(b)] corresponds to a mixture of $BaCO_3$ and CuO and a homogeneous covering with an average particle size of *ca.* 3 µm can be observed by SEM [Fig. 6(a)]. When the temperature of the thermal treatment is increased to 600 °C no significant changes were observed, either in the morphology of the deposits or in the X-ray diffraction pattern [Fig. 3(c)]. However, when the sample is treated at 700 °C both the morphology and composition show significant changes. The particle size increases to *ca.* 6 µm [Fig. 6(b)]; also, new phases: $BaSO_4$, CuO and $YBa_2Cu_3O_{7-\delta}$ can be observed in the X-ray diffraction pattern [Fig. 3(d)]. Some cracks observed in the films are most likely formed by the release of CO_2 gas. At this temperature, the $YBa_2Cu_3O_{7-\delta}$ oxide is present as a minor phase. It is important to note that below 700 °C the presence of yttrium was not detected by this X-ray technique. This implies that, even when Y_2O_3 forms (at 380 °C) it must remain as an amorphous phase(s). When the temperature is raised to 800 °C [Fig. 6(c)], the number of grain junctions increases and neck formation can be observed, even though no changes are observed in the X-ray diffraction patterns [Fig. 3(e)]. Finally,

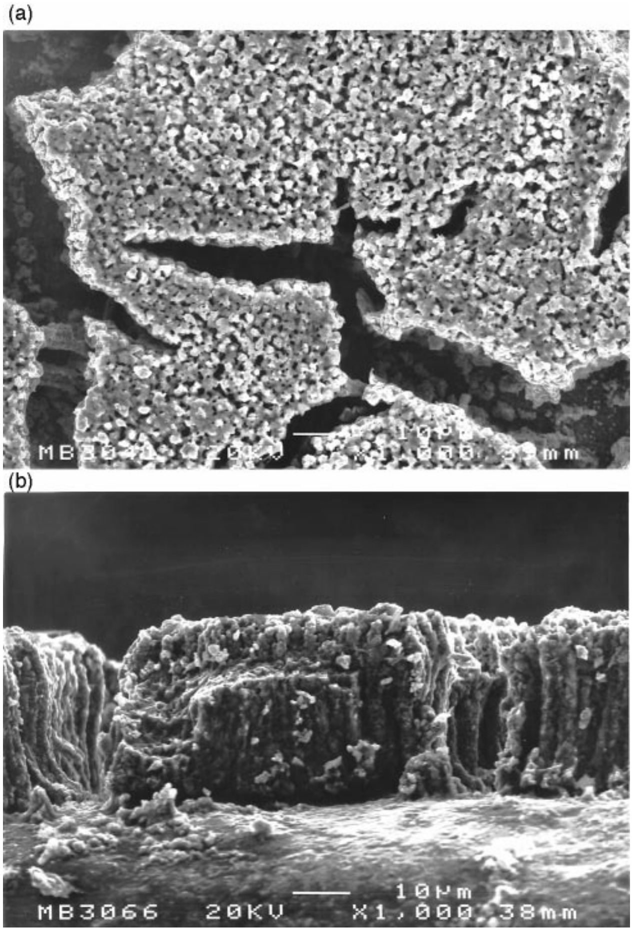

Fig. 7 Scanning electron micrographs of $YBa_2Cu_3O_{7-\delta}$ (a) top (b) side view.

when the sample is heated to 900 °C and post-annealed in O_2 at 450 °C, X-ray diffraction [Fig. 3(f)] indicates that the superconducting phase $YBa_2Cu_3O_{7-\delta}$ is the majority phase, although there are still some minor impurities of Y_2BaCuO_5, $BaSO_4$ and CuO. The presence of $BaSO_4$ was confirmed by the IR spectrum [Fig. 2(b)], where the main bands are centred at 1183, 1124 and 1085 cm^{-1}. These can be assigned to SO_4^{2-} and arise from the oxidation of dimethyl sulfone.

To summarise: (a) copper was seen by XRD as Cu and Cu_2O in the precursor film, (b) yttrium is present as the elemental form, (c) carbonates have been detected in the IR spectrum, (d) barium oxidises very readily in air and (e) at 500 °C barium carbonate is observed. We can conclude that the precursor film consists of Cu, Cu_2O, Y and $BaCO_3$.

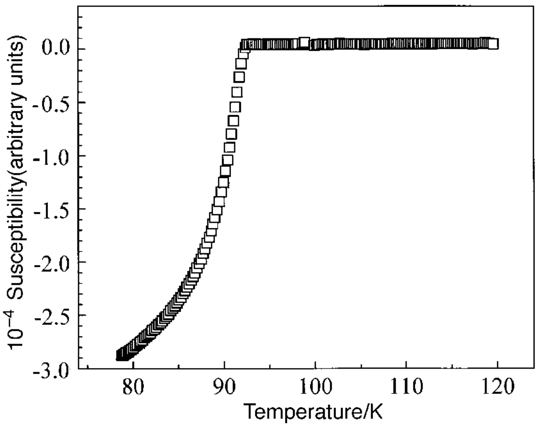

Fig. 8 Ac susceptibility measurements of a $Ag/YBa_2Cu_3O_{7-\delta}$ film.

Taking these results into account, the reactions that seem to occur during the thermal treatment of the films are given by eqn. (1)–(4):

$$Cu_2O + 0.5\ O_2 \rightarrow 2CuO\ (T \approx 260\ ^\circ C) \qquad (1)$$

$$2Y + 1.5\ O_2 \rightarrow Y_2O_3\ (T \approx 380\ ^\circ C) \qquad (2)$$

$$6CuO + 4BaCO_3 + Y_2O_3 \rightarrow 2YBa_2Cu_3O_{7-\delta} + 4CO_2\ (T \approx 750\ ^\circ C) \qquad (3)$$

$$BaCO_3 + \text{‘S’} + O_2 \rightarrow BaSO_4 + CO_2\ (T \approx 750\ ^\circ C) \qquad (4)$$

Here ‘S’ is a sulfur containing phase, possibly dimethyl sulfone, the detailed reactivity of which has not been examined.

All these reactions influence the final aspect of the film. As can be seen in Fig. 7(a), the covering has some ‘holes’. These cracks can also be observed in the side view of a film shown in Fig. 7(b). The thickness of the film is *ca.* 30 µm, which is greater than that observed before the thermal treatment. This increase can be attributed to sintering and agglomeration at high temperature; but sintering also causes cracking. It can also be seen, especially in Fig. 7(b), that the morphology of the final phase is formed by aggregated columns of $YBa_2Cu_3O_{7-\delta}$.

The average weight of the films observed after the thermal treatment was ≈15 mg cm^{-2}. Considering the thickness of the film after the thermal treatment of 30 µm, a density of 5 g cm^{-3} can be estimated. This value, below the crystal

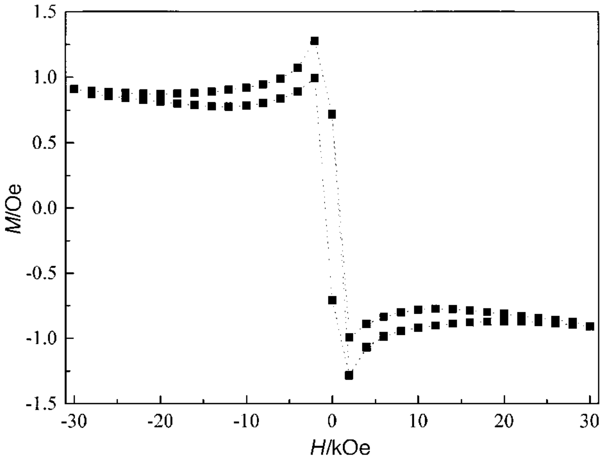

Fig. 9 Magnetic hysteresis loop measured for a $Ag/YBa_2Cu_3O_{7-\delta}$ film at 77 K.

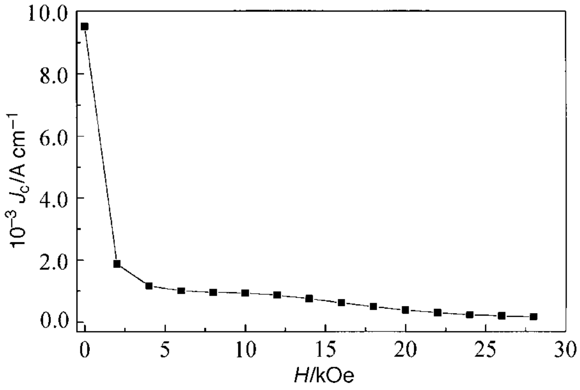

Fig. 10 Current density values at different magnetic fields for a $Ag/YBa_2Cu_3O_{7-\delta}$ film at liquid nitrogen temperature (77 K).

Table 3 Comparison of the superconducting properties of the $YBa_2Cu_3O_{7-\delta}$ films *via* electrodeposition

T_c/K	J_c/A cm^{-2}	Reference
92	51 (77 K)	11
92	2908 (4.2 K)	10
91	4000	9
91	5160	12
82	6600	13
92	9500 (77 K)	This work
92	11500 (77 K)	33

density (*ca.* 7 g cm^{-3}) of $YBa_2Cu_3O_{7-\delta}$, indicates both the lack of ideal coverage of the substrate [Fig. 7(a)] and the relatively low compactness of the film [Fig. 7(b)].

The superconducting transition temperature of the electrodeposited thick films, obtained under the conditions described in Table 1, were determined by ac magnetic susceptibility measurements. Fig. 8 shows a representative example of T_c observed in all films, $\approx$92 K. Magnetic hysteresis loops measured for these superconducting films are shown in Fig. 9 and the magnetisation critical current densities (J_c) calculated according to the Bean model are shown in Fig. 10. The J_c value calculated at 77 K and zero-field cooling was *ca.* 9500 A cm^{-2}. When a magnetic field is applied to this film this value decreases markedly, for example when a magnetic field of 2 T is applied the J_c value is reduced to *ca.* 1900 A cm^{-2}.

It should be mentioned that our J_c results are comparable, in fact somewhat better, than those obtained in previous work using electrodeposition of HTSC films (Table 3). Additionally, this value, 9500 A cm^{-2}, can be improved upon by successive electrodeposition/thermal treatments.[33] This opens up the possibility for the eventual use of this technique in practical applications.

Conclusions

$YBa_2Cu_3O_{7-\delta}$ films have been obtained by electrodeposition. The precursor film contains copper as Cu_2O and Cu; yttrium as a metal and barium appears to be present as a carbonate. These precursor phases react and at *ca.* 745 °C the formation of a $YBa_2Cu_3O_{7-\delta}$ phase is observed. Columnar growth is observed in a cross-section of the film. Under our conditions, superconducting films with $T_c \approx 92$ K and J_c values of *ca.* 9500 A cm^{-2}, at 77 K and zero field, were obtained.

Acknowledgments

This work was financially supported by CICYT Program MAT95–0809 and MAT98–0729. SEM and EDS analyses were carried out at the facilities of Microscopy Centre Luis Brú, UCM. J.G.J. wishes to thank the Basque Government/Eusko Jaurlaritza for a postdoctoral fellowship.

References

1 H. Kammerlingh-Onnes, *Akad. van Wetenschappen, Proceedings, from the section of Sciences*, Amsterdam, 1911, vol. **14**, pp. 113 and 818.

2 K. Heine, J. Tenbrink and M. Thoner, *Appl. Phys. Lett.*, 1989, **55**, 2441.

3 N. McN. Alford, S. J. Penn and T. W. Button, *Supercond. Sci. Technol.*, 1997, **10**, 169.

4 F. A. List, *Physica C*, 1998, **302**, 87.

5 A. P. Semenov, *Instrum. Exp. Tech.* (*Engl. Transl.*), 1993, **36**, 173.

6 T. J. Jackson and S. B. Palmer, *J. Phys. D: Appl. Phys.*, 1994, **27**, 1581.

7 D. L. Schulz and T. J. Marks, *Adv. Mater.*, 1994, **6**, 719.

8 D. J. Zurawski, P. J. Kulesza and A. Wieckowski, *J. Electrochem. Soc.*, 1988, **136**, 1607.

9 R. N. Bhattacharya, R. Noufi, L. L. Roybal and R. K. Ahrenkiel, *J. Electrochem. Soc.*, 1991, **138**, 1643.

10 S. Ondoño-Castillo and N. Casañ-Pastor, *Physica C*, 1997, **276**, 251.

11 S. Ondoño-Castillo, A. Fuertes, F. Pérez, P. Gómez-Romero and N. Casañ-Pastor, *Chem. Mater.*, 1995, **7**, 771.

12 R. N. Bhattacharya, P. A. Parilla, R. Noufi, P. Arendt and N. Elliott, *J. Electrochem. Soc.*, 1992, **139**, 67.

13 P. Régnier, S. Poissonnet, G. Villars and C. Louchet, *Physica C*, 1997, **282–287**, 2575.

14 M. Maxfield, H. Eckhardt, Z. Iqbal, F. Reidinger and R. H. Baughman, *Appl. Phys. Lett.*, 1989, **54**, 1932.

15 M. S. Martín-González, J. García-Jaca, E. Morán and M. Á. Alario-Franco, *J. Mater. Res.*, submitted.

16 K. A. Richardson, D. M. W. Arrigan, P. A. J. de Groot, P. C. Lanchester and P. N. Bartlett, *Electrochim. Acta*, 1996, **41**, 1629.

17 R. N. Bhattacharya, A. Duda, D. S. Ginley, J. A. DeLuca, Z. F. Ren, C. A. Wang and J. H. Wang, *Physica C*, 1994, **229**, 145.

18 R. N. Bhattacharya, P. A. Parilla and R. D. Blaugher, *Physica C*, 1993, **211**, 475.

19 M. S. Martín-González, J. García-Jaca, E. Morán and M. Á. Alario-Franco, *Physica C*, 1998, **297**, 185.

20 S. H. Pawar, M. J. Ubale and S. B. Kulkarni, *Mater. Lett.*, 1994, **20**, 279.

21 C. P. Bean, *Phys. Rev. Lett.*, 1964, **8**, 250.

22 A. P. Malozemoff, *Physical Properties of High Temperature Superconductors I*, ed. D. M. Ginsberg, World Scientific, Singapore, 1989.

23 M. S. Martín-González, J. García-Jaca, E. Morán and M. Á. Alario-Franco, *Bol. Soc. Esp. Ceram. Vidrio*, 1998, **2–3**, 200.

24 M. S. Martín-González, *Síntesis de óxidos superconductores mediante electrodeposición*, Graduation thesis, Universidad Autonoma, Madrid, 1997.

25 C. T. Cheung and E. Ruckenstein, *J. Mater. Res.*, 1989, **4**, 1.

26 K. Nakamoto, *Infrared and Raman Spectra of Inorganic and Coordination Compounds*, John Wiley & Sons, New York, 4th edn., 1986.

27 N. B. Colthup, L. H. Daly and S. E. Wiberley, *Introduction to Infrared and Raman Spectroscopy*, Academic Press, New York, 3rd edn., 1990.

28 D. Lin-Vien, N. B. Colthup, W. G. Fateley and J. G. Grasselli, *Handbook of Infrared and Raman Characteristic Frequencies of Organic Molecules*, Academic Press, New York, 1991.

29 C. Duval, *Inorganic Thermogravimetric Analysis*, Elsevier Amsterdam, 1953.

30 M. S. Martín-González, J. García-Jaca, E. Morán and M. Á. Alario-Franco, *J. Mater. Chem.*, 1999, **9**, 137.

31 A. J. Bard, *Electrochemical methods: Fundamentals and applications*, John Wiley & Sons, New York, 1980.

32 R. C. Weast, M. J. Astle and W. H. Beyer, *Handbook of Chemistry and Physics*, 67th edn., ed. R. C. Weast, CRC Press, Boca Raton, FL, 1986–1987.

33 M. S. Marbín-González, E. Morán, R. Sáez-Puche and M. Á. Alario-Franco, *Proc. MRS Fall Meeting, Boston, 1998*, in press.

Paper 8/09172B